Nano World Journal

https://doi.org/10.17756/nwj.2023-s1-035

Research Article

Open Access

Empirical Modeling of Material Removal Rate during the WEDM of Inconel 690

Atul Raj[1], Lalit K. Yadav[2*], Joy P. Misra[2] and Vikas Upadhyay[3]

[1]Department of Mechanical Engineering, NIT Kurukshetra, Haryana, India
[2]Department of Mechanical Engineering, IIT(BHU) Varanasi, Uttar Pradesh, India
[3]Department of Mechanical Engineering, NIT Patna, Bihar, India

[*]Correspondence to:
Lalit K. Yadav
Department of Mechanical Engineering,
IIT(BHU) Varanasi, Uttar Pradesh, India.
E-mail: lalitkumaryadav.rs.mec21@itbhu.ac.in

Received: November 24, 2022
Accepted: April 07, 2023
Published: April 09, 2023

Citation: Raj A, Yadav LK, Misra JP, Upadhyay V. 2023. Empirical Modeling of Material Removal Rate during the WEDM of Inconel 690. *NanoWorld J* 9(S1): S171-S175.

Published by United Scientific Group

Abstract

Material Removal Rate (MRR) is considered as the most desirable process performance measure variable of WEDM process. Variability of MRR mainly depends on the selected input process variables of WEDM process. The goal of the current research is to improve MRR by optimizing the WEDM input processing parameters. In this experiment, an empirical model of MRR was created using the following four process input variables: Power-on time, power-off time, peak current (i_p), and spark-gap voltage. Box-Behnken design (BBD) based on response surface methodology (RSM) was employed for individual responses and multi-objective/responses optimization for high-performance WEDM attributes. The nuclear and gas turbine industry favors inconel 690 workpieces. To forecast the simplified state of input process variables, RSM-based mathematical modelling is applied. Additionally, ANOVA (Analysis of Variance) is employed to identify the relevant input process variables. The results show that peak current and power-on time are the most efficient variables for achieving high MRR.

Keywords

WEDM, Inconel 690, Material removal rate, Analysis of variance

Introduction

Regardless of toughness or hardness, WEDM has developed as a special non-conventional technology for machining all varieties of conductive materials. It has a low surface roughness and can generate any complicated profile or geometry with extreme precision. A thin brass or copper wire with a thickness of 0.05 to 0.30 mm is utilized in the form of a machine tool in WEDM. Sparks generation begins in the spark gap as soon as the current starts flowing through it. Spark gap refers to the space between the two electrodes. The material is removed as a result of the discharge energy stored in the sparks [1-4]. Material removal off the work surface takes place in a very exact way. Figure 1 illustrates the fundamental process of material removal by WEDM.

For use in industries such as gas turbines, aircraft, nuclear reactors, etc., Inconel 690 is in high demand. It is an excellent material for the gas turbine and steam generator industries, as well as for the medical implant industry. Due to its unusual properties, it's a difficult-to-process material, with strong resistance to surface erosion, creep, and corrosion at high temperatures and in aqueous solution [5-8]. This study offers future researchers a course of action that they can use to better their selection and optimal setup of the input process variables. The impact of input factors on the performance of the WEDM is further understood using the ANOVA technique.

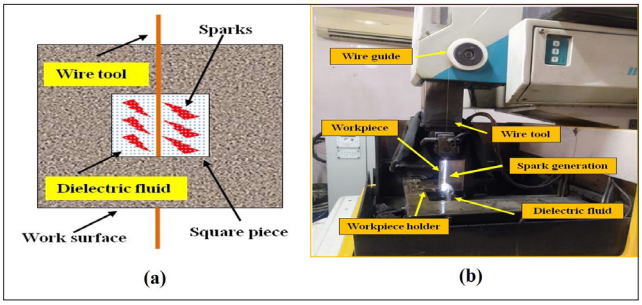

Figure 1: Fundamental process of machining by WEDM **(a)** schematic and **(b)** pictorial view.

Experimental Procedure

As shown in figure 2 the Inconel-690 is machined using an Electronica machine tool sprint cut 734 WEDM machine. Because of its remarkable qualities, broad range of applications, and ease of supply, Inconel 690 was chosen as the workpiece material. Square portions of 5 mm x 5 mm are cut from an Inconel 690 plate with dimensions of (150 mm x 150 mm x 15 mm) for experimental investigation.

P_{on}, P_{off}, I_p and S_v, are employed as input process variables in the current analysis. Each parameter has three levels, a user-defined-RSM technique is used for conducting the experimental trials. The range in which all the parameters are represented is (1, -1), with the greatest level of each parameter being 1 and the minimum level being -1 [9-12]. Table 1 illustrates the parameters' range and levels for experimental runs.

MRR is used to evaluate WEDM's performance. The experiments were conducted using BBD design based on RSM. A total of 29 runs are completed using the BBD design, with 5 center replications [13-14]. Table 2 displays the MRR experiment's combination, order, design, and outcomes.

Results and Discussion

The design, parametric arrangement, and associated experimental data for MRR are presented in table 2. Table 2 shows that the experiment with the highest MRR (9.38 mm^3/minute) was experiment 14 at the parametrical setting; S_{on}: 118 µs; S_{off}: 45 µs; I_p: 130 A; S_v: 50 V, while lowermost

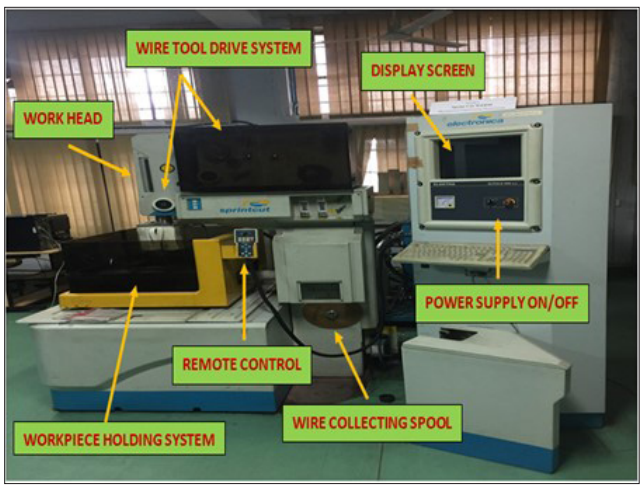

Figure 2: WEDM machine setup (Sprint cut 734).

Table 1: Levels and ranges of the process input variables.

Input process variables					
Source	**Variables**	**Unit**	**Level**		
			1	2	3
A	Power-on time (P_{on})	Mu	105	118	131
B	Power off-time (P_{off})	Mu	30	45	60
C	Peak current (I_p)	A	40	130	220
D	Spark-gap voltage (S_v)	V	20	50	80

Table 2: Design, experimental combination, and corresponding outcomes.

Run	Input process variables				MRR
	S_{on}	S_{off}	I_p	S_v	
1	118	60	40	50	1.6
2	118	30	220	50	4.84
3	131	30	130	50	6.67
4	131	45	220	50	6.86
5	118	45	40	20	4.2
6	118	45	130	50	8.26
7	118	45	130	50	8.37
8	118	30	130	20	5.14
9	118	45	220	20	6.11
10	118	60	130	80	2.42
11	118	60	130	20	7.28
12	131	45	40	50	3.98
13	105	45	40	50	1.36
14	118	45	130	50	9.38
15	118	45	130	50	8.34
16	131	60	130	50	5.55
17	118	45	220	80	6.42
18	131	45	130	80	7.47
19	118	30	130	80	5.14
20	105	45	220	50	2.41
21	131	45	130	20	6.67
22	105	60	130	50	1.27
23	118	60	220	50	5.18
24	118	45	130	50	8.38
25	105	45	130	80	1.68
26	105	30	130	50	3.83
27	118	30	40	50	4.64
28	105	45	130	20	2.23
29	118	45	40	80	2.34

MRR (1.27 mm^3/minute) was found from experiment no. 22 at parametrical setting; S_{on}: 105 µs; S_{off}: 60 µs; I_p: 130 A; S_v: 50 V. ANOVA for MRR is presented in table 3. The F-value in an ANOVA shows how much the relevant process parameter contributed. The P value must be less than 0.05 in order to confirm the significance of a process variable within a 95 percent confidence range [15-16]. The model's F-value of 19.51 shows that it is remarkably significant. In this case S_{on}, S_{off}, I_p, $S_{off} \times I_p$, $S_{off} \times S_v$, S_{on}^2, S_{off}^2, I_p^2, and S_v^2 are significant model terms.

For the current investigation, RSM-based BBD design found quadratic model to be significant. S_{on} is the most im-

Table 3: ANOVA results for MRR.

MRR							
Source	**SS**	**DF**	**MS**	**F value**	**P value**	**Importance**	**% Contribution**
Model	160.24	14	11.45	19.51	< 0.0001	Significant	95.12%
A	49.69	1	49.69	84.72	< 0.0001	Significant	29.49%
B	4.04	1	4.04	6.88	0.0200	Significant	2.39%
C	15.64	1	15.64	26.66	0.0001	Significant	9.28%
D	3.16	1	3.16	5.39	0.0358	Significant	1.87%
AB	0.52	1	0.52	0.88	0.3631	Insignificant	
AC	0.84	1	0.84	1.43	0.2521	Insignificant	
AD	0.46	1	0.46	0.78	0.3930	Insignificant	
BC	2.86	1	2.86	4.87	0.0445	Significant	1.70%
BD	5.90	1	5.90	10.07	0.0068	Significant	3.50%
CD	1.18	1	1.18	2.01	0.1784	Insignificant	
A^2	37.75	1	37.75	64.36	< 0.0001	Significant	22.40%
B^2	25.05	1	25.05	42.70	< 0.0001	Significant	14.86%
C^2	37.91	1	37.91	64.63	< 0.0001	Significant	22.50%
D^2	15.04	1	15.04	25.64	0.0002	Significant	8.92%
Residual	8.21	14	0.59				
Pure Error	0.88	4	0.22				
Cor Total	168.46	28					

portant moveable among all the input process factors. According to the ANOVA results for MRR. S_{on} (84.72) has the maximum value of F, and I_p (26.66) and S_{off} are next in line (6.88).

$$MRR = -214.912 + 3.34841 \times A + 0.58315 \times B + 0.00593264 \times C + 0.145329 \times D + 0.000625926 \times B \times C - 0.0027 \times B \times D - 0.0142756 \times A^2 - 0.0087337 \times B^2 - 0.000298467 \times C^2 - 0.00169176 \times D^2 \quad (1)$$

Figure 3 clearly shows that MRR continuously rises when P_{on} and I_p rise. For P_{off} and S_v, the phenomena are observed in reverse. As the P_{on} and I_p increase, more electrons hit the work surface in a single discharge. With each discharge, a greater amount of material is taken off the work area. Consequently, MRR increases as P_{on} and I_p increase. It is a known fact that metal gets removed from WEDM in the form of craters. Poor surface quality and a higher surface roughness score are the results of greater material removal. The ANOVA findings clearly reveal that the process parameters also interact with certain aspects of process performance, as illustrated in figure 4a: I_p-P_{off} vs MRR; figure 4b: S_v-P_{off} vs MRR. Equation 1 shows the MRR regression model R^2, which measures the degree of determination, is 0.9513. The adj. R^2 of 0.9025 is in practical covenant with the pred. R^2 of 0.7411. A signal with a sufficient precision ratio of 13.70 is present (more than 4 is needed). To find the best parameter combination for verification trials, optimization was ultimately conducted. The ideal response: Maximum MRR is 8.41 mm^3/min when P_{on}: 117 µs, P_{off}: 44 µs, I_p: 128 A, and S_v: 50 V are used.

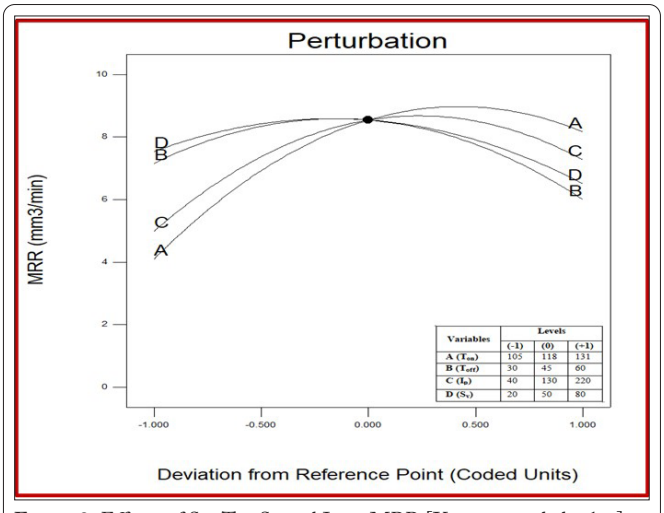

Figure 3: Effects of S_{on}, T_{off}, S_v, and I_p on MRR [X-axis in coded value].

Surface integrity analysis

Surface geometry

FE-SEM (Make: Joel, JSM-6390LV, 20.0 keV) apparatus was utilized to achieve the microstructure appearances of Inconel 690 machined through WEDM displayed in figure 5. On two square parts that have been processed using various parametric parameters (Maximum MRR, Minimum MRR), a surface integrity investigation is conducted. Study shows that several tiny fissures and craters appear to be protruding, and on the upper face of the treated surface, a few spherical

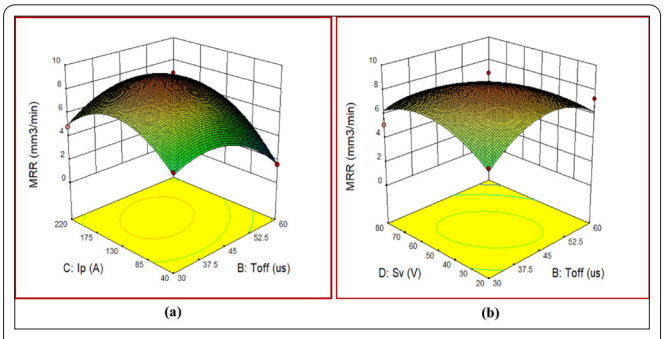

Figure 4: Interactions graphs **(a)** I_p-S_{off} vs MRR and **(b)** S_v-S_{off} vs MRR.

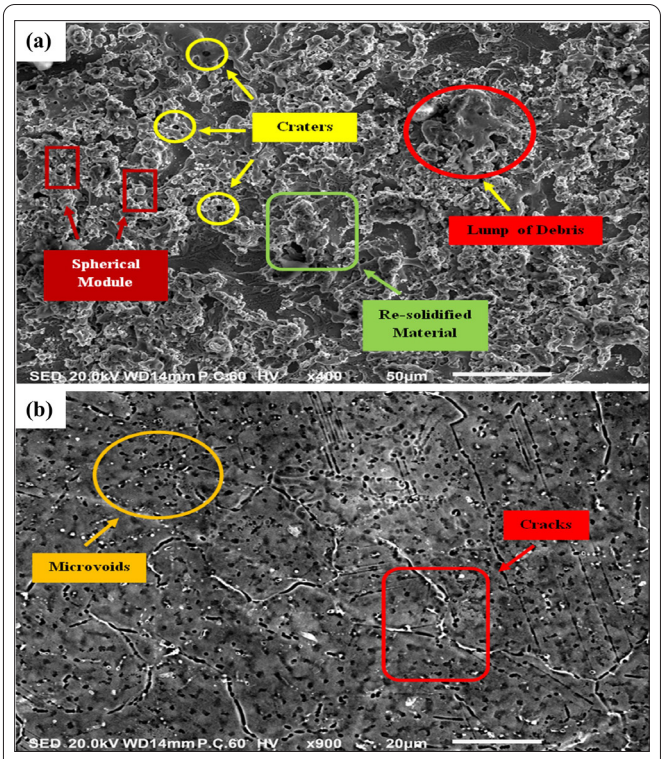

Figure 5: Machined surface SEM pictures processed at parametrical conditions: **(a)** P_{on}: 118 µs; P_{off}: 45µs; I_p: 130 A; S_v: 50 V and **(b)** P_{on}: 105 µs; P_{off}: 45 µs; I_p: 40 A; S_v: 50 V.

metal droplets have developed. There are a few rubbish lumps composed of molten metal and re-solidified stuff on the work area as well. There are also minor craters, spherical modules, a lump of debris, and resolidified material visible on the top of the machined surface.

EDS analysis

In the case of WEDM, melting and evaporation phenomena cause the substrate to be removed from the surface. It takes place in the spark gap area because of the high discharge energy emitted by the sparks. According to EDS data, wire tool residues like copper and zinc re-solidify on the top surface of the machined workpiece during the melting and evaporation process. The compositions and graphs of the recognized spectra are shown in figure 6.

Conclusion

For the current study, the BBD design of RSM technique is utilized to simultaneously optimize the parameters for the process performance variable MRR. The input variables and their interactions are modelled mathematically using quadratic regression. It is then further used to predict future MRR values. The following are the main conclusions of the current investigations.

- The most important input process variable is P_{on}, which is the case for all input process variables. Its slight variation has a big impact on how well the process works.
- P_{off} and S_v are observed to be less efficacious in comparison to P_{on} and I_p.

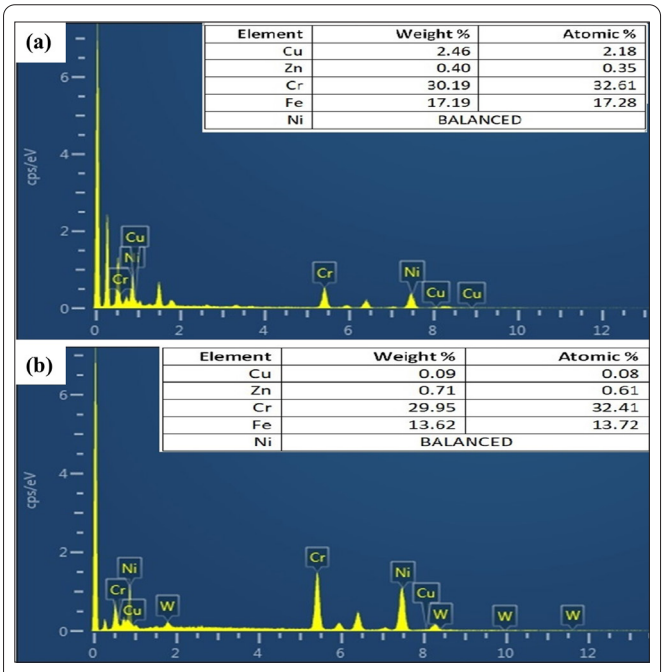

Figure 6: Machined surface EDS analysis at different parametrical conditions: **(a)** P_{on}: 118 µs; P_{off}: 45 µs; I_p: 130 A; S_v: 50 V and **(b)** P_{on}: 105 µs; P_{off}: 45 µs; I_p: 40 A; S_v: 50 V.

- The ideal input parameter setting to achieve the highest MRR is found to be P_{on}: 117, P_{off}: 44, I_p: 128 and S_v: 50.
- An analysis of surface integrity unveil that the treated superalloy's upper surface contains small craters, spherical modules, a lump of debris, and resolidified material.
- To gain a better understanding of the process, future research may take into account the tribological and microstructure examination of gears and splines produced by WEDM machining.

Acknowledgements

None.

Conflict of Interest

There is no conflict of interest to this work.

Credit Author Statement

Alok Kumar: Simulation, Data collection, Analysis; Umesh Kumar Singh: Conceptualization, Design; Avanish Kumar Dubey: Conceptualization, Design; Pratiksha: Manuscript - original draft preparation, Writing - review and editing. All the authors read and approved the manuscript.

References

1. Das A, Misra JP. 2016. Modelling and parametric optimisation of deposited layer thickness in electric discharge coating process. *Int J Surf Sci Eng* 10(3): 253-271. https://doi.org/10.1504/IJSURFSE.2016.076997
2. Bisaria H, Shandilya P. 2019. Experimental investigation on wire electric discharge machining (WEDM) of Nimonic C-263 superalloy. *Mater Manuf Process* 34(1): 83-92. https://doi.org/10.1080/10426914.201

8.1532589

3. Singh B, Misra JP. 2019. Process regulations and mechanism of WEDM of combustor material. *SAE Int J Aerospace* 12(1): 77. https://doi.org/10.4271/01-12-01-0004
4. Shandilya P, Jain PK, Misra JP. 2010. Experimental investigation during wire electric discharge cutting of SiC_p/6061 aluminum metal matrix composite. *Key Eng Mater* 450: 173-176. https://doi.org/10.4028/www.scientific.net/KEM.450.173
5. Sreenivasa Rao M, Venkaiah N. 2018. Experimental investigations on surface integrity issues of Inconel-690 during wire-cut electrical discharge machining process. *Proc Inst Mech Eng B J Eng Manuf* 232(4): 731-741. https://doi.org/10.1177/0954405416654092
6. Raj A, Misra JP, Khanduja D, Saxena KK, Malik V. 2022. Design, modeling and parametric optimization of WEDM of Inconel 690 using RSM-GRA approach. *Int J Interact Des Manuf* 1-11. https://doi.org/10.1007/s12008-022-00947-5
7. Raj A, Misra JP, Khanduja D. 2022. Performance evaluation of electro-spark eroded high-volume fraction of Cr-Fe-Ni superalloy. *Proc Inst Mech Eng C J Mech Eng Sci* 236(15): 8449-8461. https://doi.org/10.1177/09544062221081023
8. Tahir W, Jahanzaib M, Ahmad W, Hussain S. 2019. Surface morphology evaluation of hardened HSLA steel using cryogenic-treated brass wire in WEDM process. *Int J Adv Manuf Technol* 104: 4445-4455. https://doi.org/10.1007/s00170-019-04301-0
9. Raj A, Misra JP, Khanduja D. 2022. Modeling of wire electro-spark machining of inconel 690 superalloy using support vector machine and random forest regression approaches. *J Adv Manuf Sys* 21(03): 557-571. https://doi.org/10.1142/S0219686722500196
10. Balasubramaniyan C, Rajkumar K, Santosh S. 2021. Wire-EDM machinability investigation on quaternary $Ni_{44}Ti_{50}Cu_4Zr_2$ shape memory alloy. *Mater Manuf Process* 36(10): 1161-1170. https://doi.org/10.1080/10426914.2021.1905833
11. Raj A, Misra JP, Khanduja D, Upadhyay V. 2022. A study of wire tool surface topography and optimization of wire electro-spark machined UNS N06690 using the federated mode of RSM-ANN. *Int J Struct Integr* 13(2): 212-225. https://doi.org/10.1108/IJSI-09-2021-0101
12. Shandilya P, Jain PK, Jain NK. 2013. RSM and ANN modeling approaches for predicting average cutting speed during WEDM of SiC_p/6061 Al MMC. *Procedia Eng* 64: 767-774. https://doi.org/10.1016/j.proeng.2013.09.152
13. Singh B. 2021. Influences and optimization of electrical discharge machining of AISI 2205. *IOP Conf Ser Mater Sci Eng* 1116(1): 012088. https://doi.org/10.1088/1757-899X/1116/1/012088
14. Soundararajan R, Ramesh A, Mohanraj N, Parthasarathi N. 2016. An investigation of material removal rate and surface roughness of squeeze casted A413 alloy on WEDM by multi response optimization using RSM. *J Alloys Compd* 685: 533-545. https://doi.org/10.1016/j.jallcom.2016.05.292
15. Tonday HR, Tigga AM. 2017. Empirical assessment and modeling of MRR and surface roughness acquired from wire electrical discharge machining of Inconel 718. *Int J Mech Eng Technol* 8(1): 152-159.
16. Singh B, Misra JP. 2019. Surface finish analysis of wire electric discharge machined specimens by RSM and ANN modeling. *Measurement* 137: 225-237. https://doi.org/10.1016/j.measurement.2019.01.044